

Representations of Composite Braids and Invariants for Mutant Knots and Links in Chern-Simons Field Theories

P. Ramadevi, T.R. Govindarajan and R.K. Kaul

The Institute of Mathematical Sciences,
Taramani, Madras-600 113, INDIA.

Abstract

We show that any of the new knot invariants obtained from Chern-Simons theory based on an arbitrary non-abelian gauge group do not distinguish isotopically inequivalent mutant knots and links. In an attempt to distinguish these knots and links, we study Murakami (symmetrized version) r -strand composite braids. Salient features of the theory of such composite braids are presented. Representations of generators for these braids are obtained by exploiting properties of Hilbert spaces associated with the correlators of Wess-Zumino conformal field theories. The r -composite invariants for the knots are given by the sum of elementary Chern-Simons invariants associated with the irreducible representations in the product of r representations (allowed by the fusion rules of the corresponding Wess-Zumino conformal field theory) placed on the r individual strands of the composite braid. On the other hand, composite invariants for links are given by a weighted sum of elementary multicoloured Chern-Simons invariants. Some mutant links can be distinguished through the composite invariants, but mutant knots do not share this property. The results, though developed in detail within the framework of $SU(2)$ Chern-Simons theory are valid for any other non-abelian gauge group.

1 Introduction

Since the original work of Jones [1], there has been a lot of interest in polynomial invariants associated with knots [2]-[6]. Following Witten's pioneering work, numerous new knot invariants have been obtained from Chern-Simons theory based on a compact semi-simple gauge group [6]-[12]. The expectation values of the Wilson loops, which are the observables of the Chern-Simons theory, give these new knot invariants. An alternative method of obtaining these invariants involves study of N -state vertex models [13]. Representation theory of quantum groups provides yet another framework in which these invariants can be studied [14].

Two of the outstanding problems of knot theory are (i) detection of chirality of knots and links and (ii) distinguishing isotopically distinct mutant knots and links through the polynomial invariants. It is well known that Jones, HOMFLY and Kauffman/Akutsu-Wadati polynomials do not detect chirality of some of the knots. Within Chern-Simons field theoretic framework, Jones and Akutsu-Wadati polynomial correspond to $SU(2)$ theory with spin $1/2$ and spin 1 representations respectively on the Wilson lines while HOMFLY and Kauffman polynomials correspond to N -dimensional representation of $SU(N)$ and $SO(N)$ theories respectively. We have shown in our earlier work [15, 12] that the link invariants obtained by putting spin $3/2$ representation on the Wilson lines in $SU(2)$ Chern-Simons theory do detect chirality of knots upto at least 10 crossings. It appears going higher in spin, yields more powerful invariants.

It is also known that a class of knots and links, called mutants, are not distinguished by Jones, Kauffman/Akutsu-Wadati and HOMFLY polynomials. We shall demonstrate that even more general Chern-Simons invariants associated with arbitrary representations of any compact semi-simple gauge group are not powerful enough to distinguish mutants. This result follows from the braiding properties of four-point correlators of the corresponding Wess-Zumino conformal field theory on S^2 . In particular, the commonly referred class of pretzel knots (related to each other by a sequence of mutations) are not distinguished by any of these invariants.

To improve the classification scheme, we study the Murakami r -parallel version of

braids [16] in $SU(2)$ Chern-Simons theory. Instead of the original form of these composite braids, we shall develop our discussion for a symmetrized, though equivalent, version. Representations of the composite braids (symmetrized version) will be obtained in the basis of conformal blocks of $SU(2)_k$ Wess-Zumino theory. The link invariants constructed from these composite representations will be referred to as r -composite invariants in contrast to the elementary Chern-Simons invariants. In fact the r -composite invariants for knots are simply the sum of Chern-Simons invariants associated with the irreducible representations (allowed by the fusion rules of the corresponding Wess-Zumino conformal field theory) in the product of r representations living on the individual strands constituting the r -composite braid. The composite link invariants also turn out to be a weighted sum of elementary multicolour Chern-Simons invariants with the weights given in terms of the linking number and the colours of the links. We find that some mutant links are distinguished by the invariants associated with the composite braids whereas all mutant knots are not. The method is general enough to apply to Chern-Simons theory based on any arbitrary gauge group.

In sec.2, after defining the operation of mutation, we present a general proof that the field theoretic invariants do not distinguish mutants. This is done in the Chern-Simons field theory based on any arbitrary non-abelian gauge group. In sec.3, we develop the theory of r -composite braids. We present the representation theory of composite braids for $r = 2$ explicitly in the bases associated with the Hilbert space of $SU(2)$ Wess-Zumino conformal blocks. The results are then generalized to r -composite braids. In sec.4, the invariants obtained from the composite braid group representations are presented. We show that some mutant links are distinguished by the invariants of their associated composite links. In this context, pretzel links are studied as an example. In contrast, we demonstrate that the mutant knots are not detected by the composite knot invariants. Kinoshita-Terasaka and Conway knots are discussed as an example of a pair of mutant knots. We summarize the results in sec. 5.

2 Mutants and their Chern-Simons invariants

Let a link L_1 be obtained from two rooms \textcircled{S} and \textcircled{R} with two strands going in and two leaving in each of them as shown in Fig.1(a). The mutant links are obtained in the following way: (i) Remove one of the rooms, say \textcircled{R} from L_1 and rotate it through π about any one of the three orthogonal axes (γ_i) as shown in Fig.2. Clearly only two of these rotations are independent: $\gamma_3 = \gamma_1 * \gamma_2$. (ii) Change the orientations of the lines inside the rotated room $\textcircled{\gamma_i R}$ to match with the fixed orientations of the external legs of the original room \textcircled{R} . (iii) Then, replace this room back in L_1 . This yields mutant links L_2 and L_3 as shown in Fig.1(b) and (c).

It is known that isotopically distinct mutants have same Jones, HOMFLY and Akutsu-Wadati/Kauffman invariants. In fact, all the knot polynomials obtained in the Chern-Simons theory do not distinguish these mutants. To show this, observe that the link L_1 in S^3 can be obtained by gluing a 3-ball containing room \textcircled{R} as shown in Fig.3(a) with another 3-ball with oppositely oriented boundary S^2 containing room \textcircled{S} as shown in Fig.3(d). Similarly, gluing Fig.3(b) and Fig.3(c) with Fig.3(d) will give the corresponding mutant links L_2 and L_3 . Further, consider an S^3 with two balls removed from it. We place four lines, connecting the two boundaries, in it without any twist and with twists as shown in Fig.4(a), (b) and (c). Notice, gluing the three-ball of Fig.3(a) onto the manifold in Fig.4(a) does not change the three-ball. On the other hand, gluing this three-ball onto manifolds in Fig.4(b) and (c) yields the 3-balls shown in Fig.3(b) and (c) respectively. Thus gluing the manifolds of Fig.4(b) and (c) onto the manifold of Fig.3(a) is equivalent to introducing rotations γ_1 and γ_2 respectively.

To study the Chern-Simons invariants associated with mutants, we place the Wilson line operator carrying representation R of gauge group G on the strands. We are interested in evaluating the Chern-Simons functional integral over the manifolds of Figs.3 and 4. These functional integrals represent states in the Hilbert space of the 4-point correlator conformal blocks associated with 4-punctured S^2 boundaries [6]-[12]. In particular, the functional integral over the three-manifold with two boundaries and four untwisted Wilson

lines connecting these boundaries as shown in Fig.4(a) can be represented as [10]-[12]

$$\nu_1 = \sum_l |\phi_l^{side (1)}\rangle |\phi_l^{side (2)}\rangle . \quad (1)$$

Here $|\phi_l^{side (1)}\rangle$ and $|\phi_l^{side (2)}\rangle$ are the basis vectors of the two Hilbert spaces associated with two boundaries of the manifold respectively. Superscript “side” on the basis states indicate that these basis vectors are eigen states of the braiding generator b_1 and b_3 introducing half-twists in the first two or the last two strands:

$$b_1 |\phi_l^{side}\rangle = b_3 |\phi_l^{side}\rangle = \lambda_l^{(-)}(R, \bar{R}) |\phi_l^{side}\rangle . \quad (2)$$

Here the side two strands in Fig.4(a) are antiparallel and carry representation R and \bar{R} , the index l runs over all the irreducible representations in the fusion rule of $R \otimes \bar{R}$ of the corresponding Wess-Zumino model. An equivalent basis $|\phi_m^{cent}\rangle$ is one where braid generator b_2 , which introduces half-twists in the central two strands, is diagonal:

$$b_2 |\phi_m^{cent}\rangle = \lambda_m^{(+)}(R, R) |\phi_m^{cent}\rangle . \quad (3)$$

Since this refers to parallel strands in Fig.4(a) both carrying representation R , the index m refers to the allowed irreducible representations in the fusion rule $R \otimes R$ of the corresponding Wess-Zumino model. The eigenvalues $\lambda_l^{(-)}(R, \bar{R})$ and $\lambda_m^{(+)}(R, R)$ for antiparallel and parallel strands are respectively [10]:

$$\lambda_l^{(-)}(R, \bar{R}) = (-1)^\epsilon q^{C_l/2} ; \lambda_m^{(+)}(R, R) = (-1)^\epsilon q^{2C_R - C_m/2} , \quad (4)$$

where C_R , C_m and C_l are the quadratic Casimirs in the representations R , m and l respectively. Depending upon the representation l (m) occurring symmetrically or antisymmetrically in the tensor product $R \otimes \bar{R}$ ($R \otimes R$), $\epsilon = \pm 1$. Further $q = \exp 2\pi i/(k + C_v)$, where C_v is the quadratic Casimir in the adjoint representation and k is the Chern-Simons coupling.

The two bases are related by q -Racah coefficient of the quantum group G_q [17, 10]:

$$|\phi_l^{side}\rangle = \sum_m a_{lm} \begin{bmatrix} \bar{R} & R \\ R & \bar{R} \end{bmatrix} |\phi_m^{cent}\rangle . \quad (5)$$

The Chern-Simons functional integral ν_2 over the 3-manifold shown in Fig.4(b) is generated by applying braid generators b_1 and b_3^{-1} on the identity braid of Fig.4(a). Since

b_1 and b_3 commute and hence are diagonal in the same basis $|\phi_l^{side}\rangle$ and also have the same eigenvalues (2), the functional integral ν_2 for manifold of Fig.4(b) is same as that for the manifold in Fig.4(a):

$$\nu_2 = \sum_l |\phi_l^{(1)}\rangle b_1 b_3^{-1} |\phi_l^{(2)}\rangle = \nu_1 . \quad (6)$$

Though as a braid Fig.4(a) is isotopically different from Fig.4(b), the properties of the braid representations in terms of four-point conformal blocks are responsible for ν_1 to be equal to ν_2 . Such statements will not hold if we increase the number of Wilson lines in these manifolds.

In order to obtain the action of a γ_2 -mutation on any state, let us consider the Chern-Simons functional integral ν_3 corresponding to Fig.4(c). This can be obtained from the state ν_1 representing the functional integral on the manifold of Fig.4(a) by applying $b_1 b_2 b_1 b_3 b_2 b_1$ on it:

$$\nu_3 = \sum_l |\phi_l^{side(1)}\rangle b_1 b_2 b_1 b_3 b_2 b_1 |\phi_l^{side(2)}\rangle . \quad (7)$$

Now we use the fact that in this Hilbert space associated with four-punctured S^2 , $b_1 = b_3$ (2). Further, for an n -strand braid on S^2 , there is an identity $b_1 b_2 \dots b_{n-2} b_{n-1}^2 b_{n-2} \dots b_2 b_1 = 1$. This in our case $n = 4$, reduces to $b_1 b_2 b_3^2 b_2 b_1 = 1$. This makes the functional integral ν_3 to be equal to ν_1 . Hence,

$$\nu_3 = \nu_1 = \nu_2 . \quad (8)$$


Now let us turn to the Chern-Simons functional integrals for one-boundary manifolds shown in Fig.3. We shall represent them by vectors $|\psi_1\rangle$, $|\psi_2\rangle$ and $|\psi_3\rangle$ respectively. These are related to each other through the functional integrals ν_2 and ν_3 . As stated earlier, gluing the manifold of Fig.4(a) onto that of Fig.3(a) along an oppositely oriented boundary does not change the manifold. However, gluing the manifolds of Fig.4(b) and (c) onto that of Fig.3(a) changes them to the mutants depicted in Fig.3(b) and (c) respectively. These imply the following relations for the respective functional integrals:

$$|\psi_1\rangle = \nu_1 |\psi_1\rangle , \quad |\psi_2\rangle = \nu_2 |\psi_1\rangle , \quad |\psi_3\rangle = \nu_3 |\psi_1\rangle . \quad (9)$$

where the functional integrals ν_1 , ν_2 and ν_3 now refer to manifolds in Fig.4(a), (b) and

(c) with opposite orientations on the two boundaries. Thus eqn.(8) yields:

$$|\psi_1\rangle = |\psi_2\rangle = |\psi_3\rangle . \quad (10)$$

Now the Chern-Simons functional integrals over S^3 containing links L_1 , L_2 and L_3 (Fig.1), $V_R[L_1]$, $V_R[L_2]$ and $V_R[L_3]$, are given by the products of vector $\langle\Phi|$ representing the functional integral over the manifold shown in Fig.3(d) containing room  and $|\psi_1\rangle$, $|\psi_2\rangle$ and $|\psi_3\rangle$ representing Figs.3(a), (b) and (c) respectively:

$$V_R(L_1) = \langle\Phi|\psi_1\rangle, \quad V_R(L_2) = \langle\Phi|\psi_2\rangle, \quad V_R(L_3) = \langle\Phi|\psi_3\rangle. \quad (11)$$

Equation(10) then implies

$$V_R[L_1] = V_R[L_2] = V_R[L_3]. \quad (12)$$

Thus we have shown that invariants of a link and its mutants are identical for every representation R of a compact semi-simple gauge group, placed on all the Wilson lines constituting the links.

As mentioned earlier, the well-known invariants viz., Jones, HOMFLY and Kauffman polynomials are obtained from $SU(2)$, $SU(N)$ and $SO(N)$ Chern-Simons theories respectively. Also Akutsu-Wadati polynomials [13] obtained from N state vertex models correspond to $SU(2)$ with spin $N/2$ representation being placed on the knot/link. Hence the fact that all these polynomials do not distinguish mutants is a special case of the above result.

As an example, we now discuss the class of pretzel links obtained by stacking m vertical braids with arbitrary number of half-twists (a_1, a_2, \dots, a_m) as shown in Fig.5. All possible permutations \mathcal{P} of these vertical braids with different half-twists $\mathcal{P}(a_1, a_2, \dots, a_m)$ can be treated as a product of mutations of the vertical braids in pair. HOMFLY invariants for these links are shown to be same by Lickorish and Millett [18]. Our arguments above demonstrate that even other Chern-Simons invariants with same representation on the component knots are identical for these links:

$$V_R(L[a_1, a_2, \dots, a_m]) = V_R(L[\mathcal{P}(a_1, a_2, \dots, a_m)]).$$

It is appropriate at this point to mention that some mutant links can be distinguished through multicolour link invariants Ref.[10, 11] by placing different representations on the

component knots. These mutant links are those related by mutations (γ_1 , γ_2 or γ_3) in rooms containing strands carrying different representations.

3 Theory of composite braids

We saw in the last section that interesting identities of four point conformal blocks were responsible for the inability of any polynomial invariant defined from Chern-Simons theory to distinguish the mutant knots and links. Such identities are not valid for higher point conformal blocks. Composite braids when placed in a manifold with two S^2 boundaries, result in higher number of punctures on the boundaries. This raises the hope that one may be able to distinguish mutant knots and links through invariants constructed from the representations of these braids. Theory of r -parallel composite braids has been developed by Murakami [16]. We shall develop the representation theory of these composite braids in the conformal block basis.

In Murakami's construction of r -parallel version of the braids, every strand is replaced by a composite of r strands. The elementary generators b_i ($i = 1, 2 \dots n - 1$) of the braid group \mathcal{B}_n are replaced by $(n - 1)$ composite braid generators $\phi^r(b_i) \in \mathcal{B}_{rn}$ as shown in Fig.6(a) which depicts a map from $\mathcal{B}_n \rightarrow \mathcal{B}_{rn}$. In terms of the elementary braid generators b_i , the composite braid generators are given by:

$$\phi^r(b_i) = (b(ri - r + 1, ri - 1))^{(-r)} b(ri, ri + r - 1) b(ri - 1, ri + r - 2) \dots b(ri - r + 1, ri) . \quad (13)$$

where $b(i, j) = b_i b_{i+1} \dots b_j$. We shall, however, use a different construction of composite braids as shown in Fig.6(b) and (c). This one is symmetric in the two composite legs, each leg is twisted around itself by π , as against the Murakami version of Fig.6(a), where only one leg is twisted around itself by 2π . The symmetrized r -composite braid generators will be denoted by $\mathbf{B}^{(r)}$. These generators for parallel composite braids(Fig.6(b)) can be represented in terms of elementary braid generators as:

$$\begin{aligned}
\mathbf{B}^{(r)}(b_i) &= b(ri - r + 1, ri - 1)^{-1} b(ri - r + 2, ri - 1)^{-1} \dots b(ri - 1, ri - 1)^{-1} \\
&\quad b(ri + 1, ri + r - 1)^{-1} b(ri + 2, ri + r - 1)^{-1} \dots b(ri + r - 1, ri - 1)^{-1} \\
&\quad b(ri, ri + r - 1) b(ri - 1, ri + r - 2) \dots b(ri - r + 1, ri) . \quad (14)
\end{aligned}$$

where $b(i, j) = b_i b_{i+1} \dots b_j$.

The braid generators for the composite braid, like the Murakami generators [16], satisfy the braid group identities:

$$\mathbf{B}^{(r)}(b_i) \mathbf{B}^{(r)}(b_j) = \mathbf{B}^{(r)}(b_j) \mathbf{B}^{(r)}(b_i) , \quad \text{for } |i - j| > 1 \quad (15)$$

$$\mathbf{B}^{(r)}(b_i) \mathbf{B}^{(r)}(b_{i+1}) \mathbf{B}^{(r)}(b_i) = \mathbf{B}^{(r)}(b_{i+1}) \mathbf{B}^{(r)}(b_i) \mathbf{B}^{(r)}(b_{i+1}) . \quad (16)$$

The closures of composite braids give knots and links. The closure respects the invariance under Markov moves (Fig.7):

$$\text{closure}(AB) = \text{closure}(BA) , \quad (17)$$

$$\text{closure}(A \mathbf{B}^{(r)}(b_n^{\pm 1})) = \text{closure}(A) . \quad (18)$$

where A and B are elements of composite braid group \mathcal{B}_n .

The above composite braid formalism can be generalised for antiparallel strands also. This will enable us to obtain any knot or link by platting of braids [11, 12]. Such a braid is drawn in Fig.6(c). A corresponding representation in terms of the elementary braid generators can also be written down.

We shall now develop explicit representations for the composite braid generators $\mathbf{B}^{(r)}(b_i)$ in the $SU(2)$ conformal block basis. For simplicity, the discussion will be presented for composite braids made of two strands, $r = 2$. Generalizations to other values of r is straightforward.

For $r = 2$, the generators for composite parallel braids can be written as:

$$\mathbf{B}^{(2)}(b_i) = b_{2i-1}^{-1} b_{2i+1}^{-1} b(2i, 2i + 1) b(2i - 1, 2i) . \quad (19)$$

Similarly, the generators for the antiparallel composite braids are:

$$\mathbf{B}^{(2)}(b_i) = b_{2i-1} b_{2i+1} b(2i, 2i + 1) b(2i - 1, 2i) . \quad (20)$$

The representations of braid generators $\mathbf{B}^{(2)}(b_i)$ can be obtained in terms of the representations of the elementary braiding generators b_i and the duality matrix (5) relating the eigen bases of b_i and b_{i+1} in the $SU(2)$ Chern-Simons framework. Let us consider a four strand braid carrying a spin j representation. Associated composite braid with $r = 2$ will have eight elementary strands. We start with the identity operator χ_1 in a manifold with two S^2 boundaries as shown in Fig.8(a) and act on this by $\mathbf{B}^{(2)}(b_2)$ to obtain a composite braid χ_2 as shown in Fig.8(b). The Chern-Simons functional integrals over manifolds χ_1 and χ_2 can be expanded in terms of convenient conformal block bases associated with Wess-Zumino theory on the two eight-punctured S^2 boundaries in the same manner as in Ref.[11]. We shall show that the composite braid $\mathbf{B}^{(2)}(b_2)$ is diagonal in the conformal block bases $|\phi\rangle$ of $SU(2)$ Wess-Zumino theory drawn in Fig.9(a). In this figure, at every trivalent point, the various spins obey the fusion rules of the $SU(2)$ Wess-Zumino conformal field theory. Thus we write the functional integrals over manifolds χ_1 and χ_2 as:

$$\chi_1 = \sum_{l_i, m_j} |\phi_{l_1, (l_2, l_3, n_1), l_4}^{(1)}\rangle |\phi_{l_1, (l_2, l_3, n_1), l_4}^{(2)}\rangle, \quad (21)$$

$$\chi_2 = \mathbf{B}^{(2)}(b_2)\chi_1 = \sum_{l_i, m_j} |\phi_{l_1, (l_2, l_3, n_1), l_4}^{(1)}\rangle \mathbf{B}^{(2)}(b_2) |\phi_{l_1, (l_2, l_3, n_1), l_4}^{(2)}\rangle, \quad (22)$$

where the superscript (1) and (2) on the basis vectors corresponds to the two S^2 boundaries.

Writing the right-handed parallel composite braid generator explicitly in terms of the elementary braid generators, $b_3^{-1}b_5^{-1}b_4b_5b_3b_4$, its eigenvalues as indicated in Appendix, turn out to be:

$$\begin{aligned} \mathbf{B}^{(2)}(b_2) |\phi_{l_1, (l_2, l_3, n_1), l_4}\rangle &= \tilde{\lambda}_{n_1}^{(+)}(l_2, l_3) |\phi_{l_1, (l_3, l_2, n_1), l_4}\rangle, \\ \tilde{\lambda}_{n_1}^{(+)}(l_2, l_3) &= (-1)^{n_1} q^{C_{l_2} + C_{l_3} - C_{n_1}/2}. \end{aligned} \quad (23)$$

Similarly, the eigen basis for the commuting composite generators $\mathbf{B}^{(2)}(b_1)$ and $\mathbf{B}^{(2)}(b_3)$ can be shown to be that associated with the eight point conformal blocks of Fig.9(b) denoted as $|\hat{\phi}_{(l_1, l_2, m_1), (l_3, l_4, m_1)}\rangle$ with eigenvalues $\tilde{\lambda}_{m_1}^{(+)}(l_1, l_2)$ and $\tilde{\lambda}_{m_1}^{(+)}(l_3, l_4)$ for parallel composite braids, respectively.

Following Appendix, it is straightforward to work out the eigenvalues for the righthanded antiparallel composite braid operator of Fig.6(c). These eigenvalues for $\mathbf{B}^{(2)}(b_2)$ are found to be

$$\tilde{\lambda}_{n_1}^{(-)}(l_2, l_3) = (-1)^{n_1} q^{C_{n_1}/2} . \quad (24)$$

The absence of l_2 and l_3 in the expression on the right-hand side, in contrast to that for parallel braids (23) is consistent with first Reidemeister move. The eigen basis for this operator is the same as for the corresponding parallel composite braid above. Notice that these eigenvalues do not explicitly depend on the spin j of the external eight lines of the conformal bases. These depend only on the spins on the internal lines. The above discussion has been developed for symmetrized version of the composite braids (Fig.6(b),(c)). The eigenvalues of the braid matrix here have a symmetric form. For the original composite braids of Murakami (Fig.6(a)), these eigenvalues are different. For parallel (+) and antiparallel (-) composite braids, these turn out to be $\hat{\lambda}_{n_1}^{(\pm)}(l_2, l_3) = (-1)^{l_2 \pm l_3} q^{\frac{C_{l_3} - C_{l_2}}{2}} \tilde{\lambda}_{n_1}^{(\pm)}(l_2, l_3)$.

The eigen bases of odd-indexed generators $\mathbf{B}^{(2)}(b_1)$, $\mathbf{B}^{(2)}(b_3)$ and even-indexed generator $\mathbf{B}^{(2)}(b_2)$ are related by the four-point duality matrix relating the internal lines with spins l_1, l_2, n_1, l_3, l_4 in Fig.9(a) and spins l_1, l_2, m_1, l_3, l_4 in Fig.9(b):

$$\langle \hat{\phi}_{(l_1, l_2, m_1), (l_3, l_4, m_1)} | \phi_{l_1, (l_2, l_3, n_1), l_4} \rangle = a_{m_1 n_1} \begin{bmatrix} l_1 & l_2 \\ l_3 & l_4 \end{bmatrix} . \quad (25)$$

Notice again, like the eigenvalues of composite braids above, it is the duality matrix relating only the internal spins that appears here.

We have completely determined the theory of composite braid for the $r = 2$ case. Generalisation to r -composite braids with arbitrary number (n) of strands can be easily done. The relevant conformal block bases (Fig.10(a),(b)) are the extensions of the conformal blocks (Fig.9(a),(b)). The l_i ($i \in [1, n]$) are the allowed representations in the tensor product of the r spin j representations of the $SU(2)$ Wess-Zumino model. The composite strands made up of r individual strands, all carrying spin j , have been represented by thick external lines as shown in Fig.10(c).

The odd-indexed composite braid generator $\mathbf{B}^{(r)}(b_{2i+1})$ is diagonal in the $SU(2)$ conformal block basis $|\hat{\phi}\rangle$ of Fig.10(a):

$$\mathbf{B}^{(r)}(b_{2i+1})|\hat{\phi}[(l_1, l_2, m_1), s_0, (l_3, l_4, m_2), s_1, \dots, s_{i-1}, (l_{2i+1}, l_{2i+2}, m_{i+1}), \dots]\rangle = \\ \tilde{\lambda}_{m_{i+1}}(l_{2i+1}, l_{2i+2})|\hat{\phi}[(l_1, l_2, m_1), s_0, (l_3, l_4, m_2), s_1, \dots, s_{i-1}, (l_{2i+2}, l_{2i+1}, m_{i+1}), s_i, \dots]\rangle, \quad (26)$$

where the eigenvalue for parallel (+) and antiparallel (-) braid generators introducing righthanded half-twists are:

$$\tilde{\lambda}_{m_{i+1}}^{(+)}(l_{2i+1}, l_{2i+2}) = (-1)^{2l_{2i+1}-m_{i+1}} q^{C_{l_{2i+1}}+C_{l_{2i+2}}-C_{m_{i+1}}/2}, \quad (27)$$

$$\tilde{\lambda}_{m_{i+1}}^{(-)}(l_{2i+1}, l_{2i+2}) = (-1)^{m_{i+1}} q^{C_{m_{i+1}}/2}. \quad (28)$$

The eigenvalues are symmetric under interchange $l_{2i+1} \leftrightarrow l_{2i+2}$. (Notice that the l_i s are either all integer or all half-integers and hence $(-1)^{2l_i} = (-1)^{2l_j}$). The half-twist operator $\mathbf{B}^{(r)}(l_{2i+1})$, in addition to interchanging the internal labels l_{2i+1} and l_{2i+2} of the conformal block also reverses the order of the external r -legs of each composite strand (thick line) connected to these two internal lines.

The eigen basis $|\phi\rangle$ for the even indexed composite generator $\mathbf{B}^{(r)}(b_{2i})$ are diagonal in the basis of Fig.10(b):

$$\mathbf{B}^{(r)}(b_{2i})|\phi[l_1, (l_2, l_3, n_1), r_1, (l_4, l_5, n_2), r_2, \dots, r_{i-1}, (l_{2i}, l_{2i+1}, n_i), r_i, \dots]\rangle = \\ \tilde{\lambda}_{n_i}(l_{2i}, l_{2i+1})|\phi[l_1, (l_2, l_3, n_1), r_1, (l_4, l_5, n_2), r_2, \dots, r_{i-1}, (l_{2i}, l_{2i+1}, n_i), r_i, \dots]\rangle, \quad (29)$$

with eigenvalues given by eqn.(27) and (28) for parallel and antiparallel righthanded twists.

Using methods of Ref.[11], the generalised transformation matrix relating the two bases in eqns.(26, 29) (Fig.10(a) and (b)) can be seen to be:

$$\langle \hat{\phi}|\phi \rangle = \prod_i a_{r_i m_{i+1}} \begin{bmatrix} s_{i-1} & l_{2i+1} \\ l_{2i+2} & s_i \end{bmatrix} \prod_i a_{s_{i-1} n_i} \begin{bmatrix} r_{i-1} & l_{2i} \\ l_{2i+1} & r_i \end{bmatrix}, \quad (30)$$

where $r_0 = l_1$ and $s_0 = m_1$.

Equations (26 - 30) constitute the composite braid representations.

Thus it is clear that only the irreducible representation in the product of spin j carried by the individual elementary strands in a r -composite strand appear in the representation

theory of the composite braids, *i.e.*, in the braid eigenvalues (27,28) and generalised duality matrix (30).

This completes our discussion of representation theory of composite braid in the $SU(2)$ Chern-Simons framework. The formalism developed here can be extended to any compact semi-simple group. Further, we have placed the same set of r -representations in each composite strand. We could as well place different sets of r -representations on the different composite strands. Theory of such multicoloured composite braids can also be developed in a similar fashion.

4 Mutants and composite braids

After the above discussion of the representation theory of composite braids, we now take up the question whether mutant knots/links can be distinguished by invariants obtained from these new representations of the braid group. From sec.1, we know that it was the result in eqn.(8) asserting the equality of Chern-Simons functional integrals associated with Fig.4(a), (b) and (c), that was responsible for mutants to have same elementary Chern-Simons invariants. This result depended on the fact that the functional integrals over the manifolds of Fig.4(a), (b) and (c) could be written as states in the product Hilbert spaces associated with four punctured S^2 boundaries. For r -composite braids, the corresponding Hilbert spaces are those associated with boundaries with $4r$ punctures. This opens up the possibility that the invariants obtained through composite braid representations above may distinguish mutant knots/links. The manifolds corresponding to Fig.4(a), (b) and (c) are drawn with composite braids ($r = 2$) in Fig.8(a), 11(a) and (b) respectively. We shall denote the Chern-Simons functional integrals over these manifolds as N_1 , N_2 and N_3 respectively. We write down the explicit representations for them in terms of the r -composite braid representations. The functional integral N_1 associated with Fig.8(a) for r -composite braid is:

$$N_1 = \sum_{(l), m_1} |\hat{\phi}_{(l_1, l_2, m_1), (l_3, l_4, m_1)}^{(1)}\rangle |\hat{\phi}_{(l_1, l_2, m_1), (l_3, l_4, m_1)}^{(2)}\rangle, \quad (31)$$

where the conformal blocks $|\hat{\phi}\rangle$ correspond to Fig.10(a) and the superscript (1) and (2) refer to the two boundaries. The Chern-Simons functional integral N_1 here written in terms of basis in which the odd-indexed composite braid generator are diagonal is the same as χ_1 in eqn.(21) where we have represented it in a basis in which the even index generators are diagonal. The functional integral N_2 associated with Fig.11(a) can be written as:

$$\begin{aligned}
N_2 &= \sum_{(l), m_1} |\hat{\phi}_{(l_1, l_2, m_1), (l_3, l_4, m_1)}^{(1)}\rangle \mathbf{B}^{(r)}(b_1) (\mathbf{B}^{(r)}(b_3))^{-1} |\hat{\phi}_{(l_1, l_2, m_1), (l_3, l_4, m_1)}^{(2)}\rangle \\
&= \tilde{\lambda}_{m_1}^{(-)}(l_1, l_2) (\tilde{\lambda}_{m_1}^{(-)}(l_3, l_4))^{-1} |\hat{\phi}_{(l_1, l_2, m_1), (l_3, l_4, m_1)}^{(1)}\rangle |\hat{\phi}_{(l_2, l_1, m_1), (l_4, l_3, m_1)}^{(2)}\rangle, \\
&= |\hat{\phi}_{(l_1, l_2, m_1), (l_3, l_4, m_1)}^{(1)}\rangle |\hat{\phi}_{(l_2, l_1, m_1), (l_4, l_3, m_1)}^{(2)}\rangle.
\end{aligned} \tag{32}$$

Here eqn.(28) has been used. In a similar manner, the composite state N_3 associated with the r -composite braid of Fig.11(b) is:

$$\begin{aligned}
N_3 &= \sum_{(l), m_1} |\hat{\phi}_{(l_1, l_2, m_1), (l_3, l_4, m_1)}^{(1)}\rangle \mathbf{B}^{(r)}(b_2) \mathbf{B}^{(r)}(b_1) \mathbf{B}^{(r)}(b_3) \mathbf{B}^{(r)}(b_2) \\
&\quad [\mathbf{B}^{(r)}(b_3)]^{-1} [\mathbf{B}^{(r)}(b_1)]^{-1} |\hat{\phi}_{(l_1, l_2, m_1), (l_3, l_4, m_1)}^{(2)}\rangle,
\end{aligned} \tag{33}$$

The result of the composite braid $\mathbf{B}^{(r)}(b_2) \mathbf{B}^{(r)}(b_1) \mathbf{B}^{(r)}(b_3) \mathbf{B}^{(r)}(b_2) [\mathbf{B}^{(r)}(b_3)]^{-1} [\mathbf{B}^{(r)}(b_1)]^{-1}$, is simply to interchange the internal spins in the basis vector $|\hat{\phi}_{(l_1, l_2, m_1), (l_3, l_4, m_1)}^{(1)}\rangle$ to $|\hat{\phi}_{(l_4, l_3, m_1), (l_2, l_1, m_1)}^{(1)}\rangle$. This is precisely how a γ_2 -mutation would act on such a representation. This can also be seen explicitly by substituting the composite braid representation into eqn.(33). After some algebra and use of identities (A.5, A.6) from the Appendix, the following result is obtained:

$$N_3 = \sum_{(l), m_1} |\hat{\phi}_{(l_1, l_2, m_1), (l_3, l_4, m_1)}^{(1)}\rangle |\hat{\phi}_{(l_4, l_3, m_1), (l_2, l_1, m_1)}^{(2)}\rangle. \tag{34}$$

Thus clearly from eqns.(31, 32 and 34), we find :

$$N_1 \neq N_2 \neq N_3. \tag{35}$$

This result is encouraging and thus may allow us to distinguish mutants. In particular, let us consider an example of a pair of mutant links belonging to pretzel class $L_1 = L[3, 2, 2, 3]$ and $L_2 = L[3, 2, 3, 2]$ of Fig.5. These two links are related by a γ_1 -mutation. The link L_1

can be thought of as obtained by gluing two copies of the 3-ball drawn in Fig.12(a) onto each other along oppositely oriented boundaries. On the other hand, mutant link L_2 is obtained by gluing the ball of Fig.12(a) onto that in Fig.12(b). We shall study these links with the orientations as specified in these figures. We replace the strands in Fig.12(a) and (b) by composites with r elementary strands. The various braids are also changed to symmetrised composite braids. The corresponding Chern-Simons functional integral associated with these manifolds (Fig.12(a) and (b)) containing r -composite braids will be represented by vectors $|\Psi_1\rangle$ and $|\Psi_2\rangle$ respectively. Following methods of Ref.[11], these can be expressed in terms of conformal blocks associated with S^2 boundary containing $4r$ punctures. A straightforward calculation yields (after using identities A.5, A.6, and A.7):

$$|\Psi_1\rangle = \sum_{l_1, l_2, r} f(l_1, l_2, r) |\hat{\phi}_{(l_1, l_2, r), (l_2, l_1, r)}\rangle, \quad (36)$$

$$|\Psi_2\rangle = \sum_{l_1, l_2, r} f(l_1, l_2, r) |\hat{\phi}_{(l_2, l_1, r), (l_1, l_2, r)}\rangle, \quad (37)$$

where

$$f(l_1, l_2, r) = \sum_{s_1, s_2} (-1)^{2l_1+r+s_1} \frac{[2s_2+1]\sqrt{[2r+1]}}{[2l_2+1]} q^{C_{s_2}-8C_{l_1}-2C_{l_2}+\frac{3}{2}C_{s_1}} \left(a_{l_2 s_1} \begin{bmatrix} l_1 & s_2 \\ r & l_1 \end{bmatrix} \right)^2.$$

The square bracket represents the q -numbers: $[x] = (q^{x/2} - q^{-x/2})/(q^{1/2} - q^{-1/2})$. These states are related to each other by

$$|\Psi_2\rangle = N_2 |\Psi_1\rangle$$

where N_2 (Fig.11(a)) here has oppositely oriented two S^2 boundaries. It is also clear that the coefficients in the state $|\Psi_1\rangle$ is not symmetric under the interchange $l_1 \leftrightarrow l_2$. This implies: $|\Psi_1\rangle \neq |\Psi_2\rangle$ which is the reflection of the fact $N_1 \neq N_2$.

The composite invariant for the oriented link L_1 is the product of the state $|\Psi_1\rangle$ with its dual; for oriented link L_2 , it is the inner product of $|\Psi_1\rangle$ with $|\Psi_2\rangle$:

$$V_j[L_1] = \langle \Psi_1 | \Psi_1 \rangle = \sum_{l_1, l_2, r} (f(l_1, l_2, r))^2, \quad (38)$$

$$V_j[L_2] = \langle \Psi_2 | \Psi_1 \rangle = \sum_{l_1, l_2, r} f(l_1, l_2, r) f(l_2, l_1, r). \quad (39)$$

Again, clearly these are not equal: $V_j[L_1] \neq V_j[L_2]$. In particular, for $j = 1/2$ on every individual strand in the r -composite braid (Jones Polynomial), a straightforward computation yields:

$$V_{1/2}[L_1] - V_{1/2}[L_2] = q^{-4}(1 + q + q^{-1})(X - 1)^2 \quad (40)$$

where $X = (q^{-11} - q^{-10} - q^{-9} + q^{-8} - q^{-7} + q^{-5} + q^{-2})$.

Next let us take up an example of a pair of mutant knots, namely the famous 11 crossing Kinoshita-Terasaka knot and its mutant known as the Conway knot as shown in Fig.13(a) and (b). The Kinoshita-Terasaka knot K_1 can be thought of as obtained by gluing three-ball of Fig.14(b) onto that of Fig.14(c) along oppositely oriented boundaries. The Conway knot K_2 in contrast, is obtained by gluing the three-ball in Fig.14(a) onto the three-ball in Fig.14(c). The state $|\Psi_3\rangle$ associated with Fig.14(a) can be readily evaluated by the method of Ref([11]):

$$|\Psi_3\rangle = \sum_{l_1, l_2, r} A(l_1, l_2, r) |\hat{\phi}_{(l_1, l_1, r), (l_2, l_2, r)}\rangle, \quad (41)$$

where $A(l_1, l_2, r)$ is:

$$A(l_1, l_2, r) = \sum_{m, n} [2l_2 + 1] \sqrt{[2l_2 + 1][2l_1 + 1]} a_{0m} \begin{bmatrix} l_1 & l_1 \\ l_2 & l_2 \end{bmatrix} \left(\tilde{\lambda}_m^{(-)}(l_1, l_2) \right)^2 a_{0n} \begin{bmatrix} l_2 & l_2 \\ l_2 & l_2 \end{bmatrix} \\ \left(\tilde{\lambda}_n^{(+)}(l_2, l_2) \right)^{-3} a_{rm} \begin{bmatrix} l_1 & l_1 \\ l_2 & l_2 \end{bmatrix} a_{rn} \begin{bmatrix} l_2 & l_2 \\ l_2 & l_2 \end{bmatrix} a_{l_2 0} \begin{bmatrix} r & l_2 \\ l_2 & r \end{bmatrix}. \quad (42)$$

The state $|\Psi_4\rangle$ associated with Fig.14(b) is related to state $|\Psi_3\rangle$ through N_3 :

$$|\Psi_4\rangle = N_3 |\Psi_3\rangle = \sum_{l_1, l_2, r} A(l_1, l_2, r) |\hat{\phi}_{(l_2, l_2, r), (l_1, l_1, r)}\rangle. \quad (43)$$

Similar calculation for the state $|\Psi_5\rangle$ associated with Fig.14(c), yields:

$$|\Psi_5\rangle = \sum_{(l_1, l_2, r)} B(l_1, l_2, r) |\hat{\phi}_{(l_1, l_2, r), (l_1, l_2, r)}\rangle, \quad (44)$$


where $B(l_1, l_2, r)$ is given by:

$$B(l_1, l_2, r) = \sum_{(n), (m), (y), (m')} \sqrt{[2l_1 + 1][2l_2 + 1]} [2l_2 + 1] a_{0m_1} \begin{bmatrix} l_1 & l_1 \\ l_2 & l_2 \end{bmatrix} \\ a_{0m_2} \begin{bmatrix} l_2 & l_2 \\ l_2 & l_2 \end{bmatrix} \tilde{\lambda}_{m_1}^{(+)}(l_1, l_2) [\tilde{\lambda}_{m_2}^{(-)}(l_2, l_2)]^{-1} a_{n_1 m_1} \begin{bmatrix} l_1 & l_2 \\ l_1 & l_2 \end{bmatrix}$$

$$\begin{aligned}
& a_{n_2 m_2} \begin{bmatrix} l_2 & l_2 \\ l_2 & l_2 \end{bmatrix} a_{l_2 y_1} \begin{bmatrix} n_1 & l_1 \\ l_2 & n_2 \end{bmatrix} (\tilde{\lambda}_{y_1}^{(+)}(l_1, l_2))^{-1} a_{y_2 y_1} \begin{bmatrix} n_1 & l_2 \\ l_1 & n_2 \end{bmatrix} \\
& a_{n_1 m'_1} \begin{bmatrix} l_1 & l_2 \\ l_2 & y_2 \end{bmatrix} a_{n_2 m'_2} \begin{bmatrix} y_2 & l_1 \\ l_2 & l_2 \end{bmatrix} (\tilde{\lambda}_{m'_1}^{(+)}(l_2, l_2))^2 [\tilde{\lambda}_{m'_2}^{(-)}(l_1, l_2)]^{-1} \\
& a_{r m'_1} \begin{bmatrix} l_1 & l_2 \\ l_2 & y_2 \end{bmatrix} a_{r m'_2} \begin{bmatrix} y_2 & l_2 \\ l_1 & l_2 \end{bmatrix} a_{y_2 0} \begin{bmatrix} r & l_2 \\ l_2 & r \end{bmatrix} .
\end{aligned} \tag{45}$$

The composite invariant for the Kinoshita-Terasaka knot K_1 is given by the inner product of $|\Psi_4\rangle$ and $|\Psi_5\rangle$ and that for the Conway knot K_2 by the inner product of $|\Psi_3\rangle$ and $|\Psi_5\rangle$:

$$V_R[K_1] = \langle \Psi_5 | \Psi_4 \rangle = \sum_{l,r} A(l, l, r) B(l, l, r) = \langle \Psi_5 | \Psi_3 \rangle = V_R[K_2] . \tag{46}$$

Thus composite invariants do not distinguish these mutants. In fact, this is true for all mutant knots. This can be seen as follows: Consider a 3-ball containing a room  with four external legs marked as A, B, C, D as shown in the Fig.15. There are three ways in which these four legs can be connected to each other inside the room:

Case (i) A is connected to B , C is connected to D inside the room like in Fig.12(a) and (b). Then a general state associated with the Fig.15 for this case will be

$$|\tilde{\Psi}_1\rangle = \sum_{(l),r} F(l_1, l_2, r) |\hat{\phi}_{(l_1, l_2, r), (l_2, l_1, r)}\rangle , \tag{47}$$

where $F(l_1, l_2, r)$ is a function which depends on the room contained in the three-ball. In general, this function need not be invariant under interchange of l_1 with l_2 .

Case (ii) A is connected to C , B is connected to D inside the room as in Fig.14(a) and (b). Then the general state will be

$$|\tilde{\Psi}_2\rangle = \sum_{(l),r} G(l_1, l_2, r) |\hat{\phi}_{(l_1, l_1, r), (l_2, l_2, r)}\rangle . \tag{48}$$

Case (iii) A is connected to D and C is connected to B inside the room as in Fig.14(c). In this case the state will be

$$|\tilde{\Psi}_3\rangle = \sum_{(l),r} H(l_1, l_2, r) |\hat{\phi}_{(l_1, l_2, r), (l_1, l_2, r)}\rangle \tag{49}$$

Observe that, we could get knots by gluing two 3-balls such that (a) one satisfies case (i) and the other case (ii), (b) one satisfies case (i) and the other case (iii), and (c) one

satisfies case (ii) and the other case (iii). Then the composite invariants for three knots K_1 , K_2 and K_3 so constructed are:

$$\begin{aligned} V_R[K_1] &= \sum_{l,r} F(l, l, r)G(l, l, r) ; \\ V_R[K_2] &= \sum_{l,r} F(l, l, r)H(l, l, r) ; \\ V_R[K_3] &= \sum_{l,r} G(l, l, r)H(l, l, r). \end{aligned} \tag{50}$$

These knot invariants obtain contribution only from the subspace spanned by the basis vectors $|\hat{\phi}_{(l,l,r),(l,l,r)}\rangle$. Also, from eqns.(31-34), the state responsible for mutation will behave like an identity state in this subspace. *i.e.*,

$$N_1|_{l_i=l} = N_2|_{l_i=l} = N_3|_{l_i=l} . \tag{51}$$

Hence, the mutants of any knot cannot be distinguished even by composite invariants.

Clearly, the composite braid eigenvalues (27, 28) and transformation matrices (30) in this invariant subspace are the same as the eigenvalues (A.3,A.4) and duality matrices for elementary braids carrying spin l representations. Hence the r -composite invariant for a given knot is simply the sum over the Chern-Simons invariants for the irreducible representations in the product of r spin j representations. This is true not only for $SU(2)$ but, by a straightforward generalisation of above arguments, also for other compact semi-simple Lie groups. Thus this result can be stated as:

For a general gauge group G , the r -composite knot invariant associated with representation R of G is the sum of elementary Chern-Simons invariants for all irreducible representations in the product of r representations $R \otimes R \otimes \dots R$ as allowed by the fusion rules of corresponding Wess-Zumino conformal field theory.

Since elementary Chern-Simons invariants for any gauge group do not distinguish mutant knots, it is clear, not even composite invariants can do so. In particular, composite version of the HOMFLY polynomial also cannot distinguish mutant knots in contrast to results in[16].

Now let us discuss the case of mutant links. Links can be obtained by gluing each of the states corresponding to case (i), (ii) and (iii) onto its dual or mutated dual state. Notice that the state $|\tilde{\Psi}_1\rangle$ is invariant under γ_2 mutation, and the state $|\tilde{\Psi}_2\rangle$ is invariant

under γ_1 mutation. Then mutant link (if isotopically distinct) which can be constructed from $|\tilde{\Psi}_1\rangle$ ($|\tilde{\Psi}_2\rangle$) and its γ_2 (γ_1) mutated dual state cannot be distinguished by composite invariants. On the other hand mutant link obtained from $|\tilde{\Psi}_1\rangle$ ($|\tilde{\Psi}_2\rangle$) and its γ_1 (γ_2) mutated dual state can be distinguished (if isotopically distinct) by composite invariants. The example of the class of pretzel links (Fig.5) discussed above is of this type: they can be constructed by the products of $|\tilde{\Psi}_1\rangle$ with its dual and its γ_1 mutated dual respectively.

In fact the composite link invariants are related to elementary multicoloured link invariants. This follows from the fact that the eigenvalues (27, 28) of the composite braid and elementary multicoloured braid generators (A.3,A.4) are related as:

$$\tilde{\lambda}_{n_1}^{(\pm)}(l_2, l_3) = (-)^{l_2-l_3} q^{\frac{|C_{l_2}-C_{l_3}|}{2}} \lambda_{n_1}^{(\pm)}(l_2, l_3) . \quad (52)$$

Thus the composite invariant $V_j^{comp}[L]$ for a link L can be written in terms of the elementary multicolour link invariants $V_{l_1, l_2, \dots, l_m}[L]$, where l_1, l_2, \dots, l_m are the spins placed on the m component knots K_1, K_2, \dots, K_m of the link L :

$$V_j^{comp}[L] = \sum_{l_1, l_2, \dots, l_m} q^{\sum_{s,t} lk(s,t) |C_{l_s}-C_{l_t}|} V_{l_1, l_2, \dots, l_m}[L] , \quad (53)$$

The l_i span the spins of irreducible representations in the product of r spin j representations carried by the individual strands in the composite braid. Here $lk(s, t)$ is the linking number for the (K_s, K_t) pair of component knots in L . Notice that the q -independent phase factors $(-)^{l_2-l_3}$ in the eigenvalues (52) disappear in eqn.(53) because l_2-l_3 is always an integer and there are even number of crossings between any pair of linking component knots. The result in eqn.(53) generalises to invariants obtained from any arbitrary compact semi-simple group.

Though the composite braiding eigenvalues for the asymmetric and symmetric composite braids (Fig.6) are different, the composite invariants for knots and links constructed from these two types of composite braids are the same.

5 Conclusions

In this paper, we have presented a proof that the isotopically inequivalent mutant knots and links cannot be distinguished by the elementary Chern-Simons invariants associated

with the representations of any gauge group G . The proof involves the fact that independent mutations γ_1 and γ_2 on the Chern-Simons functional integral over a three-ball with four punctured S^2 boundary do not change it (eqn.10). This follows from specific braiding properties of four-point conformal blocks of the corresponding Wess-Zumino conformal field theory.

In order to explore the possibility that composite braid representations may be of help to distinguish mutant knots and links, we have developed the representation theory of such braids made up of r strands within the framework of Chern-Simons field theory. The composite representations of generators of the n -braids can be given in the basis of nr -point conformal blocks of the corresponding Wess-Zumino theory. These do not depend explicitly on the spins placed on individual strands in the r -composite braid, but depend only on the spins on the internal lines of the corresponding conformal blocks (Fig.11(a) and (b)).

The r -composite invariant for a knot carrying representation R of the group G is given by the sum of elementary Chern-Simons invariants for the knot associated with the irreducible representations in the product of r representations, $R \otimes R \otimes \dots R$, allowed by the fusion rules of the corresponding Wess-Zumino conformal field theory. Thus, it is clear that mutant knots cannot be distinguished by such composite invariants. On the other hand, we have argued that the composite invariants for a link can be written as a weighted sum of multicoloured elementary invariants (53). Therefore, some mutant links do have distinct composite invariants. These are the links related by a mutation of a four-leg room carrying strands from two distinct component knots. Specific examples discussed are the class of pretzel links. We have clearly demonstrated that the r -composite invariants associated with any representation of $SU(2)$ are indeed different. In particular, spin 1/2 composite invariants, which corresponds to Jones polynomials, distinguish these mutant links. However, links related by a mutation of a four-leg room carrying strands from the same component knot cannot be distinguished by composite invariants.

Since higher spin elementary Chern-Simons invariants tend to distinguish chirality of knots [15, 12], it is worth pointing out that the composite knot invariants will also tend to do so. However, there are exceptions. For example, the sixteen crossing knots (Fig.16(a))

and (b)) discussed in ref[19] are respectively chiral and achiral. These are also related by a mutation. Hence the chirality of knot in Fig.16(a) cannot be detected by any elementary Chern-Simons invariant, nor by any composite invariant.

Appendix

In this Appendix, following methods of ref.[11] we outline the derivation of eigenvalues of the composite braid operator for right-handed half-twists in the parallel composite ($r = 2$) strands. The operation of the symmetrized composite braid operator $\mathbf{B}^{(2)}(b_2)$ (Fig.8(b)) on the eight-point conformal block of Fig.9(a) is as follows:

$$\mathbf{B}^{(2)}(b_2)|\phi_{l_1,(l_2,l_3,n_1),l_4}\rangle = b_3^{-1}b_5^{-1}b_4b_5b_3b_4|\phi_{l_1,(l_2,l_3,n_1),l_4}\rangle. \quad (\text{A.1})$$

The basis chosen is not diagonal in the even indexed elementary generator b_4 . Using appropriate duality matrices (5), we go to its diagonal basis to operate b_4 . Then, again we have to go back to the same odd-indexed basis to operate b_3 on it. This leads to

$$\begin{aligned} b_3 b_4|\phi_{l_1,(l_2,l_3,n_1),l_4}\rangle = & \sum_{[(r),(l'),(m),n_1]} a_{m_1 n_1} \begin{bmatrix} l_1 & l_2 \\ l_3 & l_4 \end{bmatrix} a_{r_2 l_2} \begin{bmatrix} l_1 & j \\ j & m_1 \end{bmatrix} a_{r_3 l_3} \begin{bmatrix} m_1 & j \\ j & l_4 \end{bmatrix} \\ & a_{m_1, p_1} \begin{bmatrix} r_2 & j \\ j & r_3 \end{bmatrix} \lambda_{p_1}^{(+)}(j, j) a_{m_2 p_1} \begin{bmatrix} r_2 & j \\ j & r_3 \end{bmatrix} a_{r_2 l'_2} \begin{bmatrix} l_1 & j \\ j & m_2 \end{bmatrix} \\ & a_{r_3 l'_3} \begin{bmatrix} m_2 & j \\ j & l_4 \end{bmatrix} a_{m_2 n_2} \begin{bmatrix} l_1 & l'_2 \\ l'_3 & l_4 \end{bmatrix} \lambda_{l'_2}^{(+)}(j, j) |\phi_{l_1,(l'_2,l'_3,n_2),l_4}\rangle, \quad (\text{A.2}) \end{aligned}$$

where $\lambda_n^{(\pm)}(j_1, j_2)$ are the eigenvalues of elementary braiding matrices for righthanded half-twist in parallelly (+) and antiparallelly (-) oriented strands, carrying spins j_1 and j_2 , given by ([11]):

$$\lambda_n^{(+)}(j_1, j_2) = (-)^{j_1+j_2-n} q^{C_{j_1}+C_{j_2} - \frac{|C_{j_1}-C_{j_2}|}{2} - C_n/2}, \quad (\text{A.3})$$

$$\lambda_n^{(-)}(j_1, j_2) = (-)^{|j_1-j_2|-n} q^{-\frac{|C_{j_1}-C_{j_2}|}{2} + C_n/2}, \quad (\text{A.4})$$

and the four-point $SU(2)$ duality matrices $a_{ij} \begin{bmatrix} l_1 & l_2 \\ l_3 & l_4 \end{bmatrix}$ are explicitly given in Appendix I of Ref.[11].

Similarly the generators $b_3^{-1}b_5^{-1}b_4b_5$ can be applied. The following orthogonality condition and identities [11] satisfied by the q -Racah coefficients enables us to simplify the expression:

$$\sum_{m_2} a_{r_1 m_2} \begin{bmatrix} m_1 & l_1 \\ l_2 & m_3 \end{bmatrix} a_{r_2 m_2} \begin{bmatrix} m_1 & l_1 \\ l_2 & m_3 \end{bmatrix} = \delta_{r_1 r_2} , \quad (\text{A.5})$$

$$\begin{aligned} \sum_{s_1} a_{r_1 s_1} \begin{bmatrix} p_1 & j_1 \\ j_2 & p_2 \end{bmatrix} a_{r_2 s_1} \begin{bmatrix} p_1 & j_2 \\ j_1 & p_2 \end{bmatrix} (-1)^{s_1} q^{-C_{s_1}/2} \\ = (-1)^{-r_1-r_2+p_1+p_3+j_1+j_2} a_{r_1 r_2} \begin{bmatrix} j_2 & p_2 \\ j_1 & p_1 \end{bmatrix} q^{(C_{r_1}+C_{r_2}-C_{j_1}-C_{j_2}-C_{p_1}-C_{p_2})/2} , \end{aligned} \quad (\text{A.6})$$

$$\begin{aligned} \sum_{p_1} a_{l_1 p_1} \begin{bmatrix} r_1 & m_1 \\ j_1 & j_2 \end{bmatrix} a_{r_1 r_2} \begin{bmatrix} p_2 & j_3 \\ p_1 & j_2 \end{bmatrix} a_{p_1 s_1} \begin{bmatrix} r_2 & j_3 \\ m_1 & j_1 \end{bmatrix} \\ = a_{l_1 r_2} \begin{bmatrix} p_2 & s_1 \\ j_1 & j_2 \end{bmatrix} a_{r_1 s_1} \begin{bmatrix} p_2 & j_3 \\ m_1 & l_1 \end{bmatrix} . \end{aligned} \quad (\text{A.7})$$

Finally, we arrive at the simplified result for two-strand parallel composite braids:

$$\mathbf{B}^{(2)}(b_2)|\phi_{l_1,(l_2,l_3,n_1),l_4}\rangle = (-1)^{n_1} q^{C_{l_2}+C_{l_3}-C_{n_1}/2} |\phi_{l_1,(l_3,l_2,n_1),l_4}\rangle \quad (\text{A.8})$$

Starting with its representation in terms of elementary braid generators as given in eqn.(20) a similar calculation can be done for the eigen values of an antiparallel composite braid operator of Fig. 6(c).

References

- [1] V.F.R. Jones, Bull. AMS **12** (1985) 103; Ann. of Math. **128** (1987) 335.
- [2] P.Freyd, D.Yetter, J. Hoste, W.B.R.Lickorish, K.Millet and A.Ocneanu, Bull. AMS **12** (1985) 239; J.H.Przytycki and K.P.Traczyk, Kobe J. Math. **4** (1987) 115.
- [3] M.Atiyah, *The Geometry and Physics of Knots*, Cambridge Univ.Press.(1990);
- [4] L.H. Kauffman, *On Knots*, Princeton Univ. Press. (1987).
- [5] A.S. Schwarz, *New topological invariants arising in the theory of quantized fields*, Baku Int. Topological conference 1987.

- [6] E. Witten, Commun. Math.Phys **121**(1989) 351.
- [7] E. Guadagnini, M. Martellini, M. Mintchev, Phys. Lett. **B228**(1989)489; Nucl. Phys. **B330**(1990)575; P. Cotta-Ramusino, E. Guadagnini, M. Martellini, M. Mintchev, Nucl. Phys. **B330**(1990)557; E. Guadagnini, Int. Jour. Mod. Phys **A7**(1992)877; Nucl. Phys. **B375**(1992)381; Nucl. Phys. **B388**(1992)159.
- [8] K. Yamagishi, M.L. Ge and Y.S. Wu, Letts. Math. Phys. **19**(1990)15; Y. Wu and K. Yamagishi, Int. Jour. Modern Phys. **A5**(1990)1165; J.H. Horne, Nucl. Phys. **B334**(1990)669.
- [9] J.M. Isidro, J.M.F. Labastida and A.V. Ramallo, Phys. Lett. **B282**(1992)63; J.M.F. Labastida and A.V. Ramallo, Phys. Letts. **B228**(1989)214; J.M.F. Labastida, P.M. Llatas and A.V. Ramallo, Nucl. Phys. **B348**(1991)651.
- [10] R.K. Kaul and T.R. Govindarajan, Nucl. Phys. **B380**(1992)293; Nucl. Phys. **393**(1993)392; P. Ramadevi, T.R. Govindarajan, R.K. Kaul, Nucl. Phys. **402**(1993)392; Nucl. Phys. **422**(1994)291.
- [11] R.K. Kaul, Commun. Math. Phys. **162**(1994)289.
- [12] R.K. Kaul, *Knot Invariants from Quantum Field Theories* , talk at the International Colloquium on Modern Quantum Field Theory, Bombay 1994, IMSc preprint No.94/23.
- [13] Y. Akutsu and M. Wadati, J. Phys. Soc. Jpn **56**(1987)839; Y. Akutsu, T. Deguchi and M. Wadati, J. Phys. Soc. Jpn **56**(1987)3464.
- [14] A.N. Kirillov, N.Yu. Reshetikhin, LOMI Preprint E-9-88; see also in: New Developments in the theory of knots, ed. T. Kohno, Singapore: World Scientific, 1989.
- [15] P. Ramadevi, T.R.Govindarajan, R.K. Kaul :*Chirality of knots 9_{42} and 10_{71} and Chern-Simons theory*, Mod. Phys. Lett.A (in press).
- [16] J. Murakami, Osaka J. Math **26**(1989)1.

- [17] L. Alvarez Gaume, G. Gomez and G. Sierra, Phys. Letts. **B220**(1989)42. L. Alvarez Gaume, G. Sierra, *Topics in Conformal field theory*. CERN preprint TH. 5540/89.
- [18] W.B.R. Lickorish and K.C. Millett, Topology **26**(1987)107.
- [19] L.H. Kauffman, Trans. Amer. Math. Soc., **318**(1990)417.

Figure captions:

Fig.1 Mutant links.

Fig.2 Mutations $(\gamma_1, \gamma_2, \gamma_3)$ of room $\textcircled{\mathbf{R}}$.

Fig.3 Three-balls, each with four punctured S^2 boundary.

Fig.4 Diagrammatic representations of the Chern-Simons functional integrals for 3-manifolds with two boundaries: (a) ν_1 , (b) ν_2 and (c) ν_3 .

Fig.5 Pretzel link $L[a_1, a_2, \dots, a_m]$.

Fig.6 r -composite braids: (a) Murakami braid $\phi^{(r)}(b_i)$, (b) symmetrized parallel braid $\mathbf{B}^{(r)}(b_i)$ and (c) symmetrized antiparallel braid $\mathbf{B}^{(r)}(b_i)$.

Fig.7 Markov moves for composite braids.

Fig.8 Diagrammatic representations of functional integrals (a) χ_1 and (b) χ_2

Fig.9 Eight point conformal blocks bases (a) $|\phi\rangle$ and (b) $|\hat{\phi}\rangle$.

Fig.10 Eigen bases (a) $|\phi\rangle$ for odd indexed r -composite braid generator, (b) $|\hat{\phi}\rangle$ for even indexed r -composite braid generator and (c) explicit representation of the composite thick line in terms of r lines each carrying spin j .

Fig.11 Diagrammatic representations of Chern-Simons functional integrals over two-boundary manifolds N_2 and N_3 .

Fig.12 Diagrammatic representations of the states (a) $|\Psi_1\rangle$ and (b) $|\Psi_2\rangle$.

Fig.13 Eleven crossing mutants: (a) Kinoshita-Terasaka knot K_1 and (b) Conway knot K_2 .

Fig.14 Diagrammatic representations of the functional integrals over three-balls: (a) $|\Psi_3\rangle$,
(b) $|\Psi_4\rangle$ and (c) $\langle\Psi_5|$


Fig.15 A three-ball containing room  with marked points A, B, C, D on the S^2 boundary.

Fig.16 A pair of mutant knots with 16 crossings.

This figure "fig1-1.png" is available in "png" format from:

<http://arXiv.org/ps/hep-th/9412084v1>

This figure "fig1-2.png" is available in "png" format from:

<http://arXiv.org/ps/hep-th/9412084v1>

This figure "fig1-3.png" is available in "png" format from:

<http://arXiv.org/ps/hep-th/9412084v1>

This figure "fig1-4.png" is available in "png" format from:

<http://arXiv.org/ps/hep-th/9412084v1>